methylhexyl tosylate, 100814-22-0; bis(2-ethylhexyl) diselenide, 100814-23-1; bis(4-ethyl-1-methylhexyl) diselenide (isomer 1), 100814-24-2; bis(4-ethyl-1-methylhexyl) diselenide (isomer 2), 100814-25-3; bis(1-propylbutyl) diselenide, 100814-26-4; dicyclohexyl diselenide, 56592-97-3; bis(1,1-dimethylpropyl) diselenide, 100814-27-5; bis(2-ethylhexyl) triselenide (isomer 1), 100814-29-7; bis(2-ethylhexyl) triselenide (isomer 2), 100814-30-0; bis(4-ethyl-1-methylhexyl) triselenide (isomer 1), 100814-32-2; bis(4-ethyl-1-methylhexyl) triselenide (isomer 2), 100814-33-3; bis(1-propylbutyl) triselenide, 100814-34-4; dicyclohexyl triselenide, 100814-35-5; bis(1,1-dimethylpropyl) triselenide, 100814-36-6; bis(2-ethylhexyl) tetraselenide, 100814-38-8; bis(4-ethyl-1-methylhexyl) tetraselenide (isomer 1), 100814-40-2; bis(4-ethyl-1-methylhexyl) tetraselenide (isomer 2), 100814-41-3; bis(1-propylbutyl) tetraselenide, 100814-42-4; dicyclohexyl tetraselenide, 100814-43-5; bis(1,1-dimethylpropyl) tetraselenide, 100814-44-6; bis(2-ethylhexyl) pentaselenide, 100814-46-8; selenium-80, 14681-54-0.

High-Resolution ^{27}Al NMR of Aluminosilicates

E. Lippmaa,* A. Samoson, and M. Mägi

Contribution from the Institute of Chemical Physics and Biophysics of the Estonian Academy of Sciences, Tallinn 200001, USSR. *Received July 30, 1985*

Abstract: Recent advances in instrumentation and techniques have made a precise determination of isotropic chemical shifts of quadrupolar nuclei in solids practicable. Aluminum-27 chemical shifts in aluminosilicates closely parallel those of silicon-29 and display a similar dependence upon changes in both the first and second coordination spheres and the Al–O–Si bond angles.

There is considerable current interest in applying high-resolution solid-state nuclear magnetic resonance (NMR) spectroscopic techniques to the study of a number of inorganic solids, such as minerals,[1] heterogeneous catalysts, and glasses. In particular, zeolites[2,3] have been attractive objects for these studies, yielding a large share of the spectra–structure relationships established for ^{29}Si chemical shifts in solids. It has been found that a change in the silicon coordination number with oxygen from four to six leads to an about 80-ppm diamagnetic shift,[4] species with different degrees of condensation of the SiO_4 tetrahedra span a 40-ppm-shift range,[1] each substitution of silicon by aluminum in the second coordination sphere causes an analytically useful 5-ppm paramagnetic shift,[2] and the mean Si–O–T bond angle dependence is close to −0.6 ppm per degree.[5,6] Effects of a similar nature could be expected in high-resolution ^{27}Al NMR spectra as well, but their study has been hampered by the relatively small chemical shift range in aluminosilicates, poor spectral resolution, and the unavoidable second-order quadrupolar line shifts, which are very significant even at the largest commercially available magnetic field strengths (11.7 T). High-resolution NMR spectroscopy of solid samples, spun rapidly under the magic angle (54.73°) to the strong polarizing magnetic field, often dubbed magic angle spinning nuclear magnetic resonance (MAS NMR), has proved to be the method of choice for a practically complete averaging of solid-state line broadenings of spin $I = {}^1/_2$ nuclei due to chemical shift anisotropy of the powder particles. In contrast to the $I = {}^1/_2$ nuclei, magic angle spinning can only diminish and modify the second-order quadrupolar line-broadening in the NMR spectra of nonintegral spin ($I = {}^3/_2, {}^5/_2, {}^7/_2, {}^9/_2$) quadrupolar nuclei,[7-9] but it is not possible to average it to zero. The variable angle sample spinning (VASS) technique[10,11] can provide sharper lines of quadrupolar nuclei in some samples but is of limited use because it does not average other line-broadening interactions.

The first ^{27}Al $I = {}^5/_2$, 100% abundance MAS NMR measurements[7,9,12-14] immediately indicated the value of this method for the study of inorganic solids. First systematic studies[13,15] were used to establish all the main features of ^{27}Al MAS NMR spectra, useful in probing the coordination, quantity, and location of aluminum atoms in aluminosilicates. However, most of the ^{27}Al chemical shift data published correspond to the line centers of gravity and are either uncorrected or only the stationary sample or MAS NMR line widths have been used for data refinement, yielding field-dependent chemical shifts. These apparent shifts are too low (diamagnetic) if uncorrected and too high (paramagnetic) if overcorrected by using the line width dependent correction terms and assuming a purely quadrupolar yet symmetric (Gaussian) line shape.[16] These difficulties, pertinent to all quadrupolar nuclei, have blurred the structurally significant fine structure in ^{27}Al chemical shift charts, thus limiting the usefulness of ^{27}Al MAS NMR to little more than coordination number determination. In fact, no variation of ^{27}Al chemical shifts with the average T–O–T bond angle in various zeolites could be found by Nagy et al.[15]

Not only are the line positions and line shapes affected by quadrupolar interaction with the electric field gradient (EFG) at the nucleus but the same is true of line intensities. The registered ^{27}Al MAS NMR line intensities are quantitatively correct only if the radio-frequency excitation pulse is sufficiently short. For a <5% error in the central transition centerband signal intensity, the effective spin flip angle must satisfy the condition[17]

$$(I + {}^1/_2)\omega_{rf}t_1 \leq \pi/6 \qquad (1)$$

Obviously, modern high-field, high-power NMR equipment, able to handle large radio-frequency pulses, is necessary for quantitatively exact MAS NMR measurements. Many of the above mentioned limitations in ^{27}Al chemical shift measurements have likewise been overcome through development of new MAS NMR techniques. The major objectives of this study were re-

(1) Lippmaa, E.; Mägi, M.; Samoson, A.; Engelhardt, G.; Grimmer, A.-R. *J. Am. Chem. Soc.* **1980**, *102*, 4889.
(2) Lippmaa, E.; Mägi, M.; Samoson, A.; Tarmak, M.; Engelhardt, G. *J. Am. Chem. Soc.* **1981**, *103*, 4992.
(3) Klinowski, J. *Progr. NMR Spectrosc.* **1984**, *16*, 237.
(4) Lippmaa, E. T.; Samoson, A. V.; Brei, V. V.; Gorlov, Yu. I. *Dokl. AN SSSR* **1981**, *259*, 403.
(5) Thomas, J. M.; Klinowski, J.; Ramdas, S.; Hunter, B. K.; Tennakoon, D. T. B. *Chem. Phys. Lett.* **1983**, *102*, 158.
(6) Smith J. V.; Blackwell C. S. *Nature (London)* **1983**, *303*, 223.
(7) Müller, D.; Gessner, W.; Behrens, H.-J.; Scheler, G. *Chem. Phys. Lett.* **1981**, *79*, 59.
(8) Kundla, E.; Samoson, A.; Lippmaa, E. *Chem. Phys. Lett.* **1981**, *83*, 229.
(9) Freude, D.; Behrens, H.-J. *Cryst. Res. Technol.* **1981**, *16*, 36.
(10) Oldfield, E.; Schramm, S.; Meadows, M. D.; Smith, K. A.; Kinsey, R. A.; Ackerman, J. *J. Am. Chem. Soc.* **1982**, *104*, 919.
(11) Ganapathy, S.; Schramm, S.; Oldfield, E. *J. Chem. Phys.* **1982**, *77*, 4360.
(12) Mastikhin, V. M.; Krivoruchko, O. P.; Zolotovskii, B. P.; Bayanov, R. A. *React. Kinet. Catal. Lett.* **1981**, *18*, 117.
(13) Fyfe, C. A.; Gobbi, C. G.; Hartman, J. S.; Klinowski, J.; Thomas, J. M. *J. Phys. Chem.* **1982**, *86*, 1247.
(14) Meadows, M. D.; Smith, K. A.; Kinsey, R. A.; Rothgeb, T. M.; Skarjune, R. P.; Oldfield, E. *Proc. Natl. Acad. Sci. U.S.A.* **1982**, *79*, 1351.
(15) Nagy, J. B.; Gabelica, Z.; Debras, G.; Derouane, E. G.; Gilson, J.-P.; Jacobs, P. A. *Zeolites* **1984**, *4*, 133.
(16) Freude, D.; Haase, J.; Pfeifer, H.; Prager, D.; Scheler, G. *Chem. Phys. Lett.* **1985**, *114*, 143.
(17) Samoson, A.; Lippmaa, E. *Phys. Rev. B* **1983**, *28*, 6567.

0002-7863/86/1508-1730$01.50/0

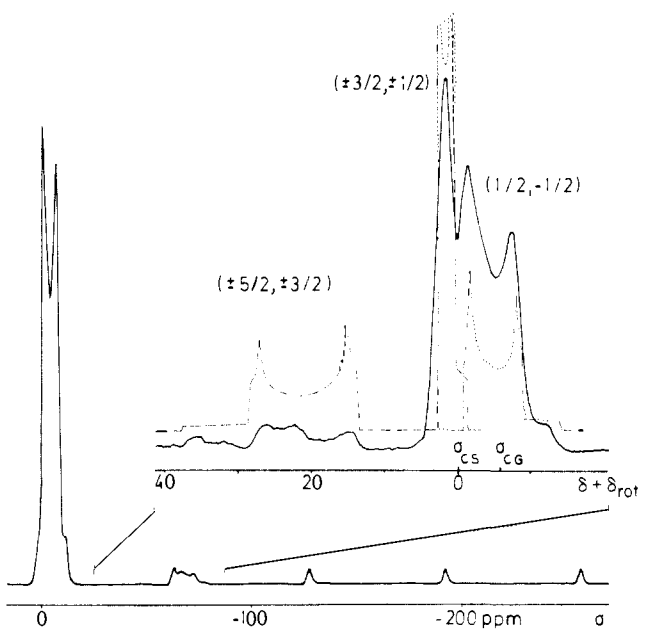

Figure 1. ^{55}Mn ($I = {}^5/_2$) MAS NMR spectrum of polycrystalline $KMnO_4$ at 49.6 MHz. The complicated structure of the first spinning sideband (solid line) is compared with the theoretical single quantum transition powder pattern line shapes (dashed lines), calculated for C_Q = 1.57 MHz and η = 0.12.[55]

finement of the ^{27}Al chemical shift data and their correlation with short-range order parameters in aluminosilicates.

Theoretical Section

MAS NMR spectra of half-integer quadrupolar nuclei do not yield the undistorted, field-independent isotropic chemical shift values directly, if the quadrupole interaction constant C_Q (product of the largest EFG tensor component eq and the nuclear quadrupole moment eQ in Hz) is not zero. The most prominent feature in the MAS NMR spectrum, the center of gravity (σ_{CG}) of the generally complicated ($+{}^1/_2, -{}^1/_2$) central transition line shape (Figure 1), is shifted from the true isotropic chemical shielding (σ_{CS}) by the second-order quadrupolar shift (σ_{QS}), which is only diminished, but not completely averaged to zero by rapid sample spinning under the magic (or any other) angle

$$\sigma_{CG}(m) = \sigma_{CS} + \sigma_{QS}(m) \tag{2}$$

The relative quadrupolar shift of the center of gravity $\sigma_{QS}(m)$ of a single quantum (m, $m-1$) transition powder pattern line shape follows from the expression for the MAS NMR centerband frequencies $\omega_{m,m-1}$ (eq 5 in ref 8) by integrating it over all possible crystallite orientations in a powder sample[18]

$$\sigma_{QS}(m) = -\frac{3}{40}\frac{C_Q^2}{\omega_L^2}\frac{I(I+1) - 9m(m-1) - 3}{I^2(2I-1)^2}\left(1 + \frac{\eta^2}{3}\right) \tag{3}$$

For the ^{27}Al MAS NMR spectrum central transition ($I = {}^5/_2$, $m = {}^1/_2$), we have from eq 3 in ppm

$$\sigma_{QS}({}^1/_2) = -6000\frac{C_Q^2}{\omega_L^2}\left(1 + \frac{\eta^2}{3}\right) \tag{4}$$

where C_Q and ω_L are both given either in Hz or in rad/s. This formula coincides with the empirical expression due to Müller[19,20] for the quadrupolar correction term.

The quadrupolar shift is fairly independent of the quadrupolar interaction asymmetry parameter η and diminishes with the second power of the Larmor frequency ω_L, but even in a 11.7-T magnetic field, where $\omega_L(^{27}Al)$ = 130.4 MHz, it may exceed 10 ppm, see

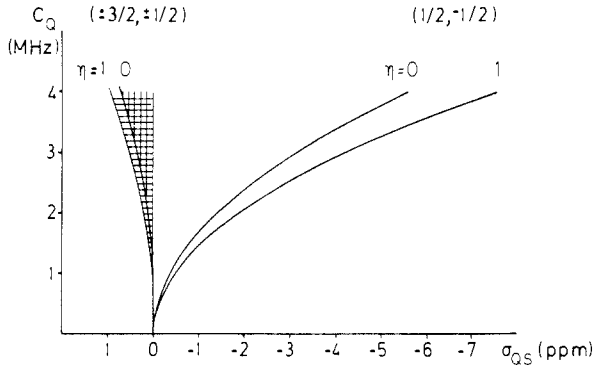

Figure 2. Second-order quadrupolar shifts of the centers of gravity of the central ($+{}^1/_2, -{}^1/_2$) and the first satellite ($\pm{}^3/_2, \pm{}^1/_2$) transitions of ^{27}Al at 130.4 MHz. Hatched areas represent the possible quadrupolar shifts $\sigma_{QS}'({}^3/_2)$, measured with the low-order rotation sidebands. The left extremes correspond to $\sigma_{QS}({}^3/_2)$.

Figure 2. Ignoring the second-order quadrupolar shifts and taking the MAS NMR line centers of gravity for the isotropic chemical shifts would introduce errors exceeding one-tenth of the whole ^{27}Al chemical shift range in aluminosilicates, large enough to swamp most structural effects in the ^{27}Al MAS NMR spectra. These errors obviously must be corrected for in all NMR experiments, including those carried out at the highest available magnetic field strengths.

If both C_Q and η are known from measurements on single crystals, then the second-order quadrupolar shift can readily be calculated from eq 3 or 4. The more accessible MAS NMR line widths, assuming Gaussian line shapes, have been used for evaluating C_Q. Indeed, if one compares eq 3 with the formulas given by Freude et al.,[16] it is apparent that the full Gaussian line width at half-height is proportional to C_Q^2 and equal to $(\ln 4)^{1/2}\sigma_{QS}({}^1/_2)$ in the absence of other line-broadening influences. However, since numerous other contributions, such as a distribution of chemical shifts due to chemical inhomogeneity, dipolar interactions, and anisotropy of magnetic susceptibility of the powder particles, also contribute to the line width, this method provides only an upper bound to the quadrupolar correction. A solely quadrupolar-broadened MAS NMR line cannot be Gaussian, but if it is, then the actual quadrupolar shift value is smaller than the correction, calculated from the line width. Stationary sample line shapes can be used for calculating the corrections only in the case of single-line spectra and are plagued by all the above mentioned line-broadening mechanisms with the addition of chemical shift anisotropy. Nevertheless, for lack of better alternatives, stationary samples have been used for the determination of C_Q and η in many cases. A typical case is the study of ^{27}Al NMR of condensed AlO_4 tetrahedra in polycrystalline aluminates.[21] This approach is justified if the ^{27}Al lines are too broad for the sample spinning rates attainable at present. Otherwise, MAS NMR spectra are clearly to be preferred.

At present there are four methods that can be used for the determination of precise isotropic chemical shift values (σ_{CS}) of half-integer quadrupolar nuclei in powder samples of solids: (1) comparison of the experimental central ($+{}^1/_2, -{}^1/_2$) transition line shapes with the calculated MAS NMR powder pattern line shapes;[8,22] (2) evaluation of the quadrupolar shifts from several MAS NMR spectra, registered at different magnetic field strengths; (3) measurement of the first or second spinning sidebands of the least shifted first satellite ($\pm{}^3/_2, \pm{}^1/_2$) transition[18] (see Figure 1); (4) determination of the first-order quadrupolar interaction parameters by fitting the experimental MAS NMR

(18) Samoson, A. *Chem. Phys. Lett.* **1985**, *119*, 29.
(19) Müller, D. *Ann. Phys.* **1983**, *39*, 451.
(20) Müller, D.; Jahn, E.; Ladwig, G.; Haubenreisser, U. *Chem. Phys. Lett.* **1984**, *109*, 332.
(21) Müller, D.; Gessner, W.; Samoson, A.; Lippmaa, E.; Scheler, G., submitted.
(22) Samoson, A.; Kundla, E.; Lippmaa, E. *J. Magn. Reson.* **1982**, *49*, 350.
(23) Lippmaa, E.; Alla, M.; Tuherm, T.; Salumäe, A. "Magnetic Resonance and Related Phenomena", Proceedings of the XXth Congress AMPERE, Kundla, E., Lippmaa, E., Saluvere, T., Eds.; Springer-Verlag: Berlin, 1979; p 99.

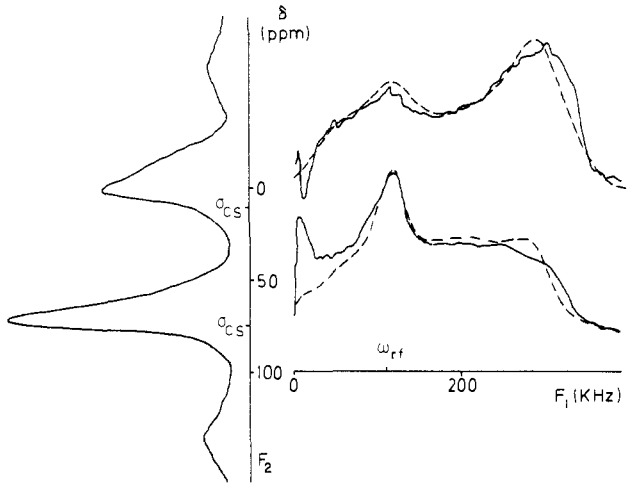

Figure 3. 2D FT MAS NMR spectrum of ^{27}Al nuclei in the layer silicate margarite at 130.4 MHz. F1 is the excitation spectra axis, providing information about the quadrupole interaction parameters through a first-order quadrupolar interaction-dependent line form and F2 is the shift axis, representing both the chemical [σ_{CS}] and the second-order quadrupolar [$\sigma_{QS}(^1/_2)$] shifts.

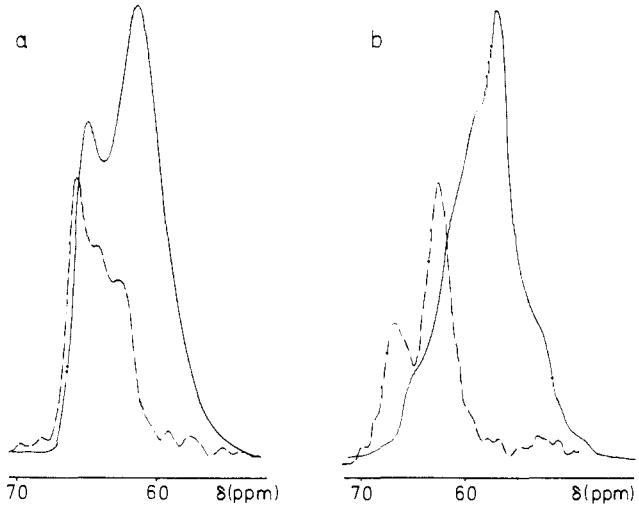

Figure 4. High-resolution MAS NMR ^{27}Al spectra of thomsonite (a) and scolecite (b). Both the central transition (bold line) and the ($^3/_2$, $^1/_2$) satellite transition (dashed line) line shapes are shown, the latter magnified and shifted by the 7-kHz sample-spinning frequency.

excitation spectra[17,24] to the numerically simulated nutation spectra (see Figure 3).

There is no general approach. While each of the methods of chemical shifts refinement has its merits, none is universally applicable. The characteristic central transition line shapes can be used with the quadrupole coupling constants C_Q in the 3–9-MHz range but are often obscured by the same line-broadening mechanisms that make measurements of quadrupolar line widths unreliable. Registration of NMR spectra at several magnetic field strengths yields useful results with smaller quadrupole coupling constants but require the use of several instruments. Measurements in lower fields unavoidably lead to diminished sensitivity and lowered resolution with the undesirable overlapping of broad lines.

In the case of sufficiently strong NMR signals, which are typical for the ^{27}Al nucleus, superior results can be achieved through the use of the ($\pm^3/_2$, $\pm^1/_2$) satellite transition sideband spectra[18] (see Figures 1 and 4). The full width of any transition of a quadrupolar nucleus follows from the second, angle-dependent term in the expression for the MAS NMR center-band frequencies (eq 5 in ref 8) and is proportional to the coefficient $6I(I+1) - 34m(m-1) - 13$. It follows immediately that the ($\pm^3/_2$, $\pm^1/_2$) satellite transition second order quadrupolar MAS NMR line width is smaller by the factor 24/7, as compared to that of the ($+^1/_2$, $-^1/_2$) central transition of a $I = {}^5/_2$ nucleus. This is a common feature of all the central and satellite transition sidebands as well. The satellite transition sidebands are caused by the first-order quadrupolar interaction, which by far exceeds the sample rotation frequency, leading to the formation of very numerous sidebands. Since only the much weaker second-order effects are involved in central transition sideband formation, the first and second sidebands of both transitions usually have comparable intensities, in marked contrast to the centerband intensity ratio, where the strong central transition resonance completely covers the weak satellite transition centerband (see Figure 1).

The second-order quadrupolar shift of the center of gravity of the whole ($\pm^3/_2$, $\pm^1/_2$) satellite transition (centerband together with all the sidebands) follows from eq 3 in ppm

$$\sigma_{QS}(^3/_2) = 750\frac{C_Q^2}{\omega_L^2}\left(1 + \frac{\eta^2}{3}\right) \qquad (5)$$

This small shift makes $\sigma_{QS}(^3/_2)$ practically equal to σ_{CS}, and the resulting minor error can easily be corrected for if C_Q and η are known (see Figure 2). The same combination of quadrupole interaction parameters is also accessible from the central transition center of gravity and it follows from eq 2, 4, and 5 that

$$\sigma_{CS} = \sigma_{CG}(^3/_2) - {}^1/_9[\sigma_{CG}(^3/_2) - \sigma_{CG}(^1/_2)] \qquad (6)$$

In practice it is impossible to determine from MAS NMR spectra the center of gravity of a whole satellite transition, split into a large number of sidebands of slightly different shapes. It follows from numerical calculations that the rotation-dependent share of the quadrupolar shift of a single low-order sideband, caused by differences in sideband formation by variously oriented crystallites at finite sample-spinning rates, does not exceed $^1/_8$ of the second-order quadrupolar line width. If the satellite transition approximate center of gravity $\sigma_{CG}'(^3/_2)$ is determined directly as the satellite center band frequency or as an average of the first or second rotation sideband centers of gravity, then $\sigma_{QS}(^3/_2)$ is still well described by eq 5. Since the low-order satellite sidebands are predominantly formed by crystallites with a smaller quadrupole splitting, these sideband line forms are deformed and $\sigma_{CG}'(^3/_2)$ shifted slightly closer to σ_{CS} than the whole-line $\sigma_{CG}(^3/_2)$ would be. Instead of (6), we have in this case a smaller correction[18]

$$\sigma_{CG}(^3/_2) > \sigma_{CS} > \sigma_{CG}(^3/_2) - {}^1/_9[\sigma_{CG}(^3/_2) - \sigma_{CG}(^1/_2)] \qquad (7)$$

The use of this expression or of the corrections shown in Figure 2 brings the precision of ^{27}Al isotropic chemical shifts in aluminosilicates in line with the ^{29}Si chemical shifts in solids (error <1 ppm).

Due to the unavoidable spread of satellite line intensity among numerous rotation sidebands, the registered MAS NMR signal is relatively weak and may be further weakened or even completely lost by fast quadrupole relaxation. Even so, it is the method of choice in the case of multiline ^{27}Al spectra, such as the ^{27}Al MAS NMR spectra of the minerals thomsonite and scolecite (see Figure 4). The central transition line shapes (solid line) are thoroughly misleading due to the near complete overlapping of several quadrupole-broadened lines, while the satellite sideband spectra (dashed line) yield all the practically undistorted isotropic ^{27}Al chemical shifts σ_{CS}. Both spectra were registered at the same magnetic field strength.

Registration of the two-dimensional arrays of MAS NMR excitation spectra is actually a nutation experiment. The precession of the ^{27}Al magnetization vector in the rotating frame is Fourier transformed to yield the spectrum of these spins in a low magnetic field, corresponding to the strength of the applied radio-frequency field. While possibly the most universal method for σ_{CS} measurement through simultaneous determination of the σ_{CG} values together with the relevant quadrupolar interaction parameters, it requires rather time-consuming and precise experiments with lengthy computations. It provides the only pos-

(24) Samoson, A.; Lippmaa, E. *Chem. Phys. Lett.* **1983**, *100*, 205.

sibility for a kind of high-resolution ^{27}Al NMR without sample spinning, applicable over a wide temperature range. ^{27}Al nuclear interactions show up in different regions of the excitation spectrum. The characteristic excitation line shapes (Figure 3) have been calculated for $I = {}^5/_2$ nuclei[24] and can be used for the determination of quadrupole interaction parameters through comparison with the experimental spectra. The technique is universally applicable with both large and small quadrupole coupling constants as long as the corresponding MAS NMR lines can be registered.

It should be noted that a $T_{1\rho}$-type process, leading to the formation of a spin-locked magnetization during the long radio-frequency excitation pulse, may result in spurious peaks at $F_1 = 0$ in the 2D spectrum. The zero-frequency peaks shown in Figure 3 can, however, be very significantly reduced by applying immediately after the strong excitation pulse, but before data acquisition, an additional 90° phase-shifted weak radio-frequency pulse. The unwanted spin-locked component of the central transition magnetization can be reduced to close to zero by a suitable choice of the amplitude (about $^1/_{10}$ of the excitation pulse) and length of this phase-shifted pulse. The use of ±90° phase alternation between successive scans serves to remove similar effects due to the magnetization oscillating along the strong polarizing magnetic field.

Experimental Section

All ^{27}Al MAS NMR spectra were recorded in a 11.7-T magnetic field at 130.4 MHz on a modified Bruker AM-500 high-resolution NMR spectrometer. For chemical shift refinement, some measurements were repeated at 93.8 MHz on a slightly modified Bruker CXP-200 solid-state NMR spectrometer equipped with a 8.45-T Oxford Instruments superconducting magnet. Special probes, free of aluminum background signal, were built for both instruments. A double air-bearing design with cylindrical side-supported rotors[23,25] provided for stable sample spinning without rotor wobble or fluctuations around the precise magic angle setting. This system allows efficient averaging of the large first-order quadrupolar line-broadenings, present in the NMR spectra of $I = 1$ spin nuclei[26] and in the satellite transition spectra of $I = {}^3/_2, {}^5/_2, \ldots$ spin nuclei.[22] The cylindrical rotors, machined from an organic aluminum-free polymer, could be stably rotated at speeds up to 9 kHz. This rotation rate in a 11.7-T magnetic field is sufficient for the registration of high-resolution MAS NMR spectra of ^{27}Al nuclei subjected to up to $C_Q = 9$ MHz quadrupolar couplings. The high rotation rates also provide for efficient suppression of dipolar interactions with the abundant $I = {}^1/_2$ nuclei (^1H) and the possible paramagnetic impurities.

Between 100 and 10000 free induction decays (FID) were accumulated at a repetition time of 0.1 to 1 s. An Aspect-2000 computer was used for the 1D FT experiments, but the 2D-FT experiments were done with an Aspect-3000 computer. For quantitative accuracy short radio-frequency pulses with the spin flip angle satisfying condition 1, were used.

In order to register the two-dimensional 2D FT MAS NMR spectra, an Amplifier Research L-200 broadband power amplifier was added to the AM-500 NMR spectrometer and provided the necessary 140-kHz amplitude of the radio-frequency excitation field strength. These nutation spectra were recorded by accumulating a few hundred FID signals, each recorded after full recovery of the ^{27}Al equilibrium magnetization, while the radio-frequency pulse lengths t_1 were increased between the FID accumulations by 1-μs increments from 1 to 128 μs. The FID signal damping time in the t_1 dimension was typically 30 μs which, apart from the quadrupolar interactions, was also caused by insufficient amplitude stability of the broadband amplifier used. This fast decay diminished spectral resolution in the excitation spectra but being much shorter than the sample rotation period allowed the use of stationary energy levels in the calculation of the theoretical excitation spectra used for the estimation of the quadrupolar interaction parameters. This approximation, though in general not necessarily a good one, is further justified by the strength of the radio-frequency excitation field used, $\omega_{rf} \gg \omega_{rot}$, which guarantees magnetization nutation in the spin space at a rate greatly exceeding that of sample spinning. A 2D FT over the spin excitation time t_1 and the free induction decay time t_2 provided all necessary data for the determination of the isotropic chemical shift values σ_{CS} (see Figure 3).

All solid-state ^{27}Al isotropic chemical shifts σ_{CS} are given in ppm with paramagnetic shifts positive and are referenced to an external 3M solution of $Al(NO_3)_3$ in water. The shift measurement error is <1 ppm and there is no essential difference between ^{27}Al shifts measured from $Al(NO_3)_3$ and $AlCl_3$ solutions.

With the exception of zeolites, all the samples examined were natural minerals[27] of good quality, almost free of sideband-generating paramagnetic impurities and with such a high content of the major constiuent that no impurity signals could be detected in the ^{27}Al MAS NMR spectra. All samples were examined as finely ground powders. A Fritsch Pulverisette mill with tungsten carbide and zirconium oxide mortars was used.

Table I. ^{27}Al Chemical Shifts[a] in Al_2SiO_5 Polymorphs

compound	δ_{CS} Al[4]	δ_{CS} Al[5]	δ_{CS} Al[6]	C_Q, MHz	η	ref
sillimanite	64.5			6.77	0.532	28
			4.0	8.93	0.462	
andalusite		36.0		5.9	0.69	29
			b	15.7	0.08	
kyanite			7.5	6.53	0.59	30
			5.0	3.70	0.89	
			b	9.37	0.38	
			b	10.04	0.27	

[a] In ppm from external 3 M $Al(NO_3)_3$ in water. [b] MAS NMR measurements not possible at present.

Table II. Four- and Six-Coordinate ^{27}Al Chemical Shifts[a] of Q^3(3 Si) Units in Layer Aluminosilicates

compound	δ_{CS} Al[4]	δ_{CS} Al[6]	$\sigma_{CG}(^1/_2)$[b]	C_Q, MHz
pennine	72 ± 2		69	2.8 ± 0.4
		10 ± 1	9.5	1.4 ± 0.2
muscovite	72 ± 1		70	2.1 ± 0.3
		5 ± 1	3	2.2 ± 0.3
margarite[c]	76 ± 3		69	4.2 ± 0.5
		11 ± 4	−3	6.3 ± 1.0
xantophyllite	76 ± 4		72.5	2.8 ± 0.4
		11 ± 1	9.5	2.0 ± 0.3

[a] In ppm from external 3 M $Al(NO_3)_3$ in water. [b] ±0.5 ppm. [c] See Figure 3.

Table III. Four-Coordinate ^{27}Al Chemical Shifts[a] of Q^4(4 Si) Units in Framework Aluminosilicates

compound	δ_{CS}[b]	$\sigma_{CG}(^1/_2)$[c]	method of shift refinement	θ', deg	ref
mordenite	55.8	55.3	*d*	153.7	44
gismondine	56.4	55.5	*e*		
NaA zeolite	59.2	58.7	*e*, *f*	148.3	45
analcime	59.4	58.5	*e*	144.3	46
chabazite	59.4	58.4	*e*	145.4	47
gmelinite	59.9	59.0	*d*	143.3	48
microcline	60.9	57.9	*e*	141.6	49
nepheline	61.0	60.1	*e*	142.0	50
	63.5	63.1	*e*	138.5	
NaX, Y zeolites	62.8	61.3	*f*	140.0	51, 52
albite	63.0	58.0	*g*	136.2	38, 49
natrolite	64.0	63.0	*g*	136.0	39, 53
sodalite	64.5	64.2	*e*	138.2	54
thomsonite	62.7	61.2	*e*	139.4	42
	64.4	61.2	*e*	135.2	
	65.8	64.4	*e*	133.6	
scolecite	62.5	57.0	*e*	137.6	41
	66.4	57.0	*e*	132.7	

[a] In ppm from external 3 M $Al(NO_3)_3$ in water. [b] ±1 ppm. [c] ±0.5 ppm. [d] Repeated measurements at different magnetic field strengths. [e] Registration of the $(\pm^3/_2, \pm^1/_2)$ satellite transition sidebands. [f] Registration of the $(\pm^1/_2, -^1/_2)$ central transition nutation spectra. [g] Curve fitting with the calculated MAS NMR quadrupolar line shapes.

Results and Discussion

All ^{27}Al chemical shifts together with the quadrupole interaction parameters or the quadrupolar shifts are presented in the Tables

(25) Lippmaa, E.; Alla, M.; Salumäe, A.; Tuherm, T. USP 4254373, Mar. 3, 1981.

(26) Eckman, R.; Alla, M.; Pines, A. *J. Magn. Reson.* **1980**, *41*, 440.

(27) Mägi, M.; Lippmaa, E.; Samoson, A.; Engelhardt, G.; Grimmer, A.-R. *J. Phys. Chem.* **1984**, *88*, 1518.

I–III. A study of the Al_2SiO_5 polymorphs (Table I) shows both the most prominent shift–structure relationships as well as limitations of the MAS NMR method. The ^{27}Al chemical shift refinement of these minerals is based on quadrupole interaction parameters from independent single-crystal measurements.[28-30] Two six-coordinate aluminum sites in kyanite and one in andalusite could not be resolved and measured in powder samples even in a 11.7-T magnetic field, using the fastest sample spinning rate (9 kHz) available at present. The extremely strong quadrupole couplings C_Q exceeded 9 MHz in all three cases. All these difficulties are still more pronounced in lower fields and at lower sample spinning rates. Many published Si/(Si + Al) and in particular the Al(4)/Al(6) ratios may therefore be seriously in error.

It is evident from Table I that the ^{27}Al chemical shift is a monotonous function of the coordination number, decreasing by about 30 ppm per bond with oxygen. This dependence is of the same nature and only slightly less pronounced than that found in ^{29}Si solid-state high-resolution NMR spectra. In contrast to silicon, five-coordinate aluminum is quite widespread in aluminosilicates. The chemical shift of five-coordinate aluminum in andalusite is a nearly perfect average of the tetrahedral and octahedral aluminum resonances in sillimanite. Five-coordinate aluminum sites are also reversibly formed during dehydration of kaolinite clays and thus make up a distinct feature in the ^{27}Al MAS NMR spectra of some industrial catalysts.

Of all the numerous silicon species with different states of condensation of the SiO_4 tetrahedra and aluminum substitution in the second coordination sphere $Q^n(m\text{Al})$, $n \geq m$, only those satisfying the Loewenstein rule that forbids immediate contact between aluminum tetrahedra[31] have aluminum-centered counterparts in aluminosilicates, thus limiting the condition $n \geq m$ to $n = m$. If we take, in full analogy with the silicon nomenclature,[1] that n denotes the number of attached tetrahedra and m shows the extent of substitution in the second coordination sphere, then we have Q^4(4 Si) and Q^3(3 Si) as the main aluminum-centered structural units in framework silicates and layer silicates, respectively. The Q^2(2 Si) and Q^1(1 Si) units have been found in soluble tetramethylammonium aluminosilicates[32,33] but are quite rare. The Q^n (n = 0 to 4) units, representing single tetrahedra (Q^0), aluminum tetrahedra in pairs (Q^1), chains and rings (Q^2), branching sites (Q^3), and three-dimensional framework structures in aluminates (Q^4), span a chemical shift range from 62 to 85 ppm, but all these groups of interconnected aluminum tetrahedra cannot be distinguished due to a practically complete overlap of the ^{27}Al chemical shift ranges.[21] With the possible exception of bicchulite, these structural units have not been found in zeolites and other aluminosilicates.

Difference between the Q^3(3 Al) and Q^4(4 Al) ^{29}Si chemical shift range midpoints is about 10 ppm, and effects of roughly the same size could be expected in the ^{27}Al NMR spectra. Only the actual isotropic ^{27}Al chemical shifts can be used to establish chemical shift ranges for the only structurally important aluminum-centered units, Q^3(3 Si) and Q^4(4 Si).

Both layer and framework aluminosilicates were studied in order to establish the influence of the second coordination sphere around aluminum upon its chemical shifts. The results are given in Tables II and III.

^{27}Al chemical shifts of the layer aluminosilicates were refined by the nutation method. Because of overlapping of lines from two satellite transitions, corresponding to two different aluminum sites, use of broad-line NMR spectroscopy or NQR spectra for the determination of quadrupole interaction parameters would have been very difficult or impossible. Damping of the transverse magnetization during spectrum excitation was fast (<30 μs) and mainly caused by an inhomogeneous spread of quadrupole interaction parameters in the aluminosilicate layers. The ^{27}Al 2D FT MAS NMR spectra of margarite display, nevertheless, a clear distinction between the two aluminum sites and allow one not only to establish the C_Q values but also to put tentative limits to the EFG tensor asymmetry parameter, $\eta = 0.5 \pm 0.3$ for the tetrahedral and $\eta = 0.1 \pm 0.1$ for the octahedral aluminum.

The ^{27}Al isotropic chemical shift range of the Q^3(3 Si) groups in layer silicates is 70–80 ppm (see Table II), distinctly more paramagnetic than the 55–68 ppm ^{27}Al chemical shift range found for the tetrahedral Q^4(4 Si) units that make up the structure of framework aluminosilicates (see Table III). It is important to note the close relatedness of ^{27}Al and ^{29}Si chemical shifts—both are more paramagnetic in the aluminum-rich margarite and xantophyllite.

These ^{27}Al chemical shift ranges are somewhat different from those based on earlier data, uncorrected for the second-order quadrupolar shifts, and may well be too narrow because of insufficient data. They are, however, in good agreement with the corrected results of other studies of layer silicates.[35-37] The first two studies were carried out in a 7-T field and the correction terms that can be calculated from the line widths and must be added to the ^{27}Al chemical shift values published are of the order of 10 ppm. The necessary corrections constitute at least a few ppm in the 11.7-T field used by Oldfield et al.[37]

The ^{27}Al isotropic chemical shifts of framework aluminosilicates, presented in Table III, were determined with a <1 ppm error. The most convenient shift refinement method in this case proved to be registration of the $(\pm^3/_2, \pm^1/_2)$ satellite transition spectra. Only in a few cases was it prohibited, possibly through fast quadrupole relaxation. Refinements of the ^{27}Al chemical shifts of the NaA, NaX, and NaY zeolites with small quadrupole interaction constants were based on the 2D nutation spectra, yielding $C_Q = 1.1 \pm 0.1$ MHz, $\eta = 0.75 \pm 0.25$ for NaA and $C_Q = 2.0 \pm 0.1$ MHz, $\eta = 0.50 \pm 0.20$ for NaX and NaY, respectively. The satellite sideband spectra were also measured for NaA zeolite and yielded the same results. The ^{27}Al chemical shifts of NaX and NaY zeolites were independent of the Si/Al ratio in the 1.14–2.85 range. The quadrupolar shifts of ^{27}Al in albite and natrolite were calculated with use of the published quadrupole interaction parameters.[38,39] Assignment of the two inequivalent ^{27}Al lines with a 3:4 intensity ratio in nepheline is based on the Al/Si distribution, which predicts a 65:80 ratio.[40] According to the crystallographic data, scolecite[41] contains two and thomsonite[42] three inequivalent aluminum sites, which could not be resolved in the ^{27}Al central transition MAS NMR spectra. All aluminum resonances are nevertheless resolved in the satellite sideband spectra, see Figure 4, which make an accurate ^{27}Al chemical shift measurement possible. The ^{27}Al and ^{29}Si chemical shifts in framework aluminosilicates with a Si/Al = 1 ratio, i.e., with strictly alternating SiO_4 and AlO_4 tetrahedra, are again correlated. Shielding decreases for both nuclei from gismondine and NaA zeolite to sodalite.

The above mentioned correlation is closely related to the linear dependence of ^{29}Si chemical shifts on the mean bond angles θ = (Si–O–Si,Al) in framework silicates.[5,43] In the first approximation this dependence can be described as linear[43]

$$\delta_{CS}(\text{Si}) = -0.619\theta - 18.7 \text{ (ppm)} \quad (8)$$

with $r = 0.97$.

(28) Raymond, M.; Hafner, S. S. *J. Chem. Phys.* **1970**, *53*, 4110.
(29) Hafner, S. S.; Raymond, M.; Ghose, S. *J. Chem. Phys.* **1970**, *52*, 6037.
(30) Hafner, S. S.; Raymond, M. *Am. Mineral.* **1967**, *52*, 1632.
(31) Loewenstein, W. *Am. Mineral.* **1954**, *39*, 92.
(32) Mueller, D.; Hoebbel, D.; Gessner, W. *Chem. Phys. Lett.* **1981**, *84*, 25.
(33) Engelhardt, G.;. Hoebbel, D.; Tarmak, M.; Samoson, A.; Lippmaa, E. *Z. Anorg. Allg. Chem.* **1982**, *484*, 22.
(34) Engelhardt, G.; Radeglia, R. *Chem. Phys. Lett.* **1984**, *108*, 271.
(35) Thompson, J. G. *Clay Miner.* **1984**, *19*, 229.
(36) Sanz, J.; Serratosa, J. M. *J. Am. Chem. Soc.* **1984**, *106*, 4790.
(37) Kinsey, R. A.; Kirkpatrick, R. J.; Hower, J.; Smith, K. A.; Oldfield, E. *Am. Mineral.* **1985**, *70*, 537.
(38) Brun, E.; Hafner, S. S.; Hartmann, P. *Helv. Phys. Acta* **1960**, *33*, 495.
(39) Petch, H.; Pennington, K. *J. Chem. Phys.* **1962**, *36*, 1216.
(40) Brinkman, D.; Ghose, S.; Laves, F. *Z. Kristallogr.* **1972**, *135*, 208.
(41) Joswig, W.; Bartl, H.; Fuess, H. *Z. Kristallogr.* **1984**, *166*, 219.
(42) Alberti, A.; Vezzalini, G.; Tazzoli, V. *Zeolites* **1981**, *1*, 91.
(43) Engelhardt, G.; Radeglia, R. *Chem. Phys. Lett.* **1984**, *108*, 271.

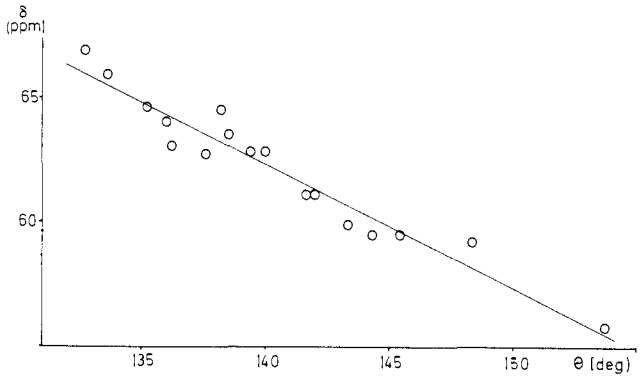

Figure 5. The dependence of ^{27}Al chemical shifts on the mean [Al–O–Si] bond angles in framework aluminosilicates.

A very similar relationship holds between the ^{27}Al chemical shifts (see Table III) and the mean bond angles $\theta' = \langle Al–O–Si \rangle$ as well (see Figure 5). The values of mean $\langle Al–O–Si \rangle$ bond angles presented in Table III are based on the latest crystallographic studies available to us. For natrolite and scolecite they were derived from data, presented in ref 41 and 53. A linear regression, based on 17 data points, yields

$$\delta_{CS}(Al) = -0.50\theta' + 132 \text{ (ppm)} \quad (9)$$

with $r = 0.95$. A tentative assignment of ^{27}Al resonances in scolecite and thomsonite, based on the mean bond angles, fits this correlation.

A very similar correlation with a −0.61 ppm/deg increment between the ^{27}Al chemical shifts and the mean bond angles has been found in $AlPO_4$ polymorphs.[20] The actual ^{27}Al chemical shifts, refined through MAS NMR curve fitting and stationary sample measurements at a low field, were used.

It appears to be well established now that accurate isotropic, field-independent solid-state ^{27}Al chemical shifts can be determined with modern instrumentation and the new techniques even in powder samples and should be used in all MAS NMR experiments. There is much analogy with the ^{29}Si chemical shifts which display a closely similar dependence upon changes in both the first and second coordination sphere and in correlations with the mean bond angles.

Acknowledgment. We are grateful to Dr. G. Engelhardt (Central Institute of Physical Chemistry, Berlin) for graciously providing us with many of the aluminosilicate samples used.

Registry No. Al, 7429-90-5.

(44) Schlenker, J. L.; Pluth, J. J.; Smith, J. V. *Mat. Res. Bull.* **1979**, *14*, 849.
(45) Gramlich, V.; Meier, V. M. *Z. Kristallogr.* **1971**, *133*, 134.
(46) Ferraris, G.; Jones, D. W. Yerkess, J. *Z. Krtstallogr.* **1972**, *135*, 240.
(47) Smith, J. V.; Knowles, C. R.; Rinaldi, F. *Acta Crystallogr.* **1964**, *17*, 374.
(48) Fischer, K. *N. Jahrb. Mineral. Monatsh.* **1966**, 1.
(49) Smith, J. V. "Feldspar Minerals"; Springer-Verlag: Berlin, 1974; Vol. 1.
(50) Hahn, T.; Buerger, H. J. *Z. Kristallogr.* **1955**, *106*, 308.
(51) Olson, D. H. *J. Phys. Chem.* **1970**, *74*, 2758.
(52) Mortier, W. J.; Bosmans, H. J. *J. Phys. Chem.* **1971**, *75*, 3327.
(53) Pechar, F. *Acta Crystallogr.* **1981**, *B37*, 1909.
(54) Hassan, I.; Grundy, H. D. *Acta Crystallogr.* **1984**, *B40*, 6.
(55) Wadsworth, M.; France, P. *J. Magn. Reson.* **1983**, *51*, 424.

Intramolecular Hydrogen Bonding as Reflected in the Deuterium Isotope Effects on Carbon-13 Chemical Shifts. Correlation with Hydrogen Bond Energies

Jacques Reuben

Contribution No. 1863 from Hercules Incorporated, Research Center, Wilmington, Delaware 19894. *Received September 16, 1985*

Abstract: The carbon-13 resonances of atoms bearing phenolic or enolic hydroxyl groups, that are engaged in intramolecular hydrogen bonds, experience large ($^2\Delta$ may exceed 1 ppm) upfield deuterium isotope effects. The magnitude of the two-bond isotope effect, $^2\Delta$, correlates with the hydrogen bond energy as obtained from the hydroxyl proton chemical shift. In the conjugated systems investigated in this work, the isotope effects extend over several (up to six) chemical bonds. The signs and magnitudes of the long-range isotope effects are related to molecular structure.

Hydrogen bonding is an important phenomenon ubiquitous in cellular matter.[1] Intramolecular hydrogen bonding plays a key role in maintaining the functional structure of biological macromolecules. Recently a possible relation between intramolecular hydrogen bonds and activity of anthracycline antitumor agents has been indicated.[2] Manifestations of hydrogen bonding can be observed by almost all of the available spectroscopic techniques.[3] The isotopic multiplets in carbon-13 NMR spectra of partially deuterated molecules comprise a new spectroscopic approach to the elucidation of molecular structure, dynamics, and equilibria.[4] In a continuation of the efforts[5,6] directed toward unraveling the information content of these multiplets, a series of substances with hydroxyl groups engaged in intramolecular hydrogen bonds were investigated. Reported here are the results of this investigation.

Carbon atoms in the vicinity of partially deuterated hydroxyl groups exhibit multiplet structure in the proton-decoupled car-

(1) Watson, J. D. "Molecular Biology of the Gene"; W. A. Benjamin, Inc.: New York, 1965; Chapter 4.
(2) Ashnagar, A.; Bruce, J. M.; Dutton, P. L.; Prince, R. C. *Biochim. Biophys. Acta* **1984**, *801*, 351-359.
(3) Vinogradov, S. N.; Linnell, R. H. "Hydrogen Bonding"; Van Nostrand-Reinhold Co.: New York, 1971.
(4) For a review see: Hansen, P. E. *Annu. Rep. NMR Spectrosc.* **1983**, *15*, 105-234.
(5) Reuben, J. *J. Am. Chem. Soc.* **1983**, *105*, 3711-3713; **1984**, *106*, 2461-2462; **1985**, *107*, 1433-1435.
(6) Reuben, J. *J. Am. Chem. Soc.* **1984**, *106*, 6180-6186; **1985**, *107*, 1747-1755; **1985**, *107*, 1756-1759.

0002-7863/86/1508-1735$01.50/0